JOURNAL OF MATERIALS SCIENCE 29 (1994) 5309–5315

Fabrication and microstructural evaluation of ZrB_2/ZrC/Zr composites by liquid infiltration

SANG KUK WOO, CHONG HEE KIM
Department of Ceramic Science and Engineering, Korea Advanced Institute of Science and Technology, 373-1 Kusong-dong, Yusong-Gu, Taejon 305-701, Korea

EUL SON KANG
Advanced Technology Research Centre, Agency for Defense Development, Yusong P. O. Box 35, Taejon 305-600, Korea

The microstructure of ZrB_2/ZrC/Zr composites was examined using scanning electron microscopy, optical microscopy, and X-ray diffraction techniques. Dense ZrB_2/ZrC/Zr composites could be fabricated by the reaction sintering of molten zirconium with ZrB_2 preform. The composites were made by infiltration of molten zirconium into ZrB_2 preform, which contained 0–40 vol % B_4C, at 1900 °C for 10 min. The average grain size of ZrB_2 in the reaction-sintered composites decreased slightly with an increase in the volume fraction of the B_4C. The volume fraction of the solid increased with further increase of B_4C contents. The mechanical properties were measured in accordance with B_4C contents. The composites exhibited a four-point bending strength of up to 570 MPa and a fracture toughness of up to 11.5 MPa $m^{1/2}$.

1. Introduction

High-temperature materials based on zirconium diboride are of considerable interest to industry because of their high melting points, high strength, high corrosion resistance, high hardness, high electrical conductivity, and oxidation resistance [1]. However, to ensure that these favourable properties are attained in actual components, it is necessary to develop economic techniques for the manufacture of parts of high relative density from these materials, because their strength and corrosion resistance are very adversely affected by excessive porosity in sintered bodies [2]. The hot pressing is not particularly suitable for this application, because its processing capacity is limited and the preparation of pure materials presents difficulties.

Therefore, the application of these compacts may require alloying or composite structures. Compacts prepared by mixing powders of zirconium diboride and metal have been tried [3, 4], but they present difficulties in manufacturing the dense bodies.

Recently, to solve these problems, reaction-based processes have been introduced. Processes based on reactions between a porous solid and an infiltrating liquid phase share the near-net shape and near-net dimension capabilities of gas-phase reaction bonding, as well as the reduced processing temperature relative to solid-state sintering [5, 6]. In addition, they have significant advantages in the processing rates and material densities that are achievable. The prototype of liquid-phase reaction-bonded materials is reaction-bonded silicon carbide (RBSC), first prepared by Popper [7], as a means of bonding silicon carbide grains into a refractory body. RBSC is typically fabricated by infiltrating molten silicon into a compacted body of the α-SiC filler and graphite. The molten silicon rises through the porous compact by capillary action, converting the graphite to new SiC. The new SiC begins to fill up the spaces between the α-SiC filler by means of solution precipitation. The final microstructure was originally described by both Popper [7] and Forrest *et al.* [8] as consisting of large grains (10–20 μm) of α-SiC (the original silicon carbide) bonded together by fine β-SiC which was produced from the reaction of carbon with liquid silicon.

Most recently, Johnson *et al.* reported the formation of zirconium diboride platelet-reinforced zirconium carbide matrix materials by the direct reaction of molten zirconium [9, 10]. Upon subsequent heating above the melting temperature of zirconium, the metal reacts and infiltrates into the bed of boron carbide, forming the products ZrB_2 and ZrC. The reported properties of this material were excellent and included values for the room-temperature flexural strength of 800–900 MPa and the fracture toughness of 16–18 MPa $m^{1/2}$. However, the reaction of zirconium with pure B_4C preform presents some problems. First, the reaction between pure molten zirconium and boron carbide preform occasionally occurred only at their contact points and could not progress further: the so-called reaction choking or freeze choking. Secondary, a gradient in grain size was observed in the reaction products because the reaction rate was very slow.

In the present study, ZrB_2/ZrC/Zr composites were made by infiltrating molten zirconium into ZrB_2–B_4C preform at 1900 °C for 10 min. The effects of B_4C

0022–2461

content in the preform on the final microstructure of the composites were evaluated. In particular, shape, distribution and content relationships of the constituent phases were observed. The reaction mechanism will be briefly presented here. In addition, the mechanical properties of composite specimens were investigated. Both bending and fracture toughness testing were used to characterize the mechanical properties.

2. Experimental procedure

The raw materials were ZrB_2 and B_4C (Hermann C. Starck, Berlin, German), and zirconium (Armco Products, Inc., Ossing, NY, USA). The ZrB_2 powder, together with B_4C and polyethyleneglycol (PEG, 4000) were mixed in a polypropylene bottle for 1 h in acetone and then dried at room temperature. The mixed powders were granulated using a 60 mesh sieve and die-pressed to form pellets 1 in (2.54 cm) inner diameter. The binder in the preform was burnt out in an electric furnace in a nitrogen atmosphere at 600 °C, which removed more than 99% of the binder. The specimens were heated in graphite crucibles in a induction furnace to the 1900 °C reaction temperature in vacuum, and the temperature was measured pyrometrically to $\pm$ 25 °C through a quartz window in the furnace.

The densities of the resulting specimens were measured by Archimedes' principle using water. The phases of the specimens were identified using X-ray diffraction of polished cross-sections perpendicular to the growth direction, with a Rigaku RTP 300RC. All specimens were examined by both secondary electron and backscattered electron imaging in a Philips XL-30. Specimens for microscopic examinations were polished with 0.25 μm diamond paste, photomicrographs of the polished sections were obtained after etching for 5 s using $HF:HNO_3:H_2O$ solution in the ratio of 2:3:95. Reaction-bonded specimens were cut from each billet (16 mm long by 3 mm wide and 2 mm thick) with a diamond saw. One face of these bars was carefully polished down to 3 μm with diamond paste and its edges were bevelled. The flexural strength was measured under four-point bending (12 mm outer span, 6 mm inner span) with a 1127 Instron machine. The fracture toughness was determined using the Vickers indentation technique with a Akashi MVK-E.

3. Results and discussion

The optical microscopy images of etched surfaces of $ZrB_2/ZrC/Zr$ composite fabricated by the reaction process are shown in Fig. 1 as a function of B_4C content. The images showed that the structure was dense and that there were few or no macro-pores. All materials appeared uniform and isotropic throughout the cross-sections observed perpendicular to the growth direction. Fig. 2 shows the back-scattered electron images (BEI) of the ZrB_2–15 vol % B_4C preform infiltrated by zirconium. The white matrix is free zirconium, the grey parts show newly formed ZrC grains which are embedded in free zirconium, and the dark parts show original and newly formed ZrB_2.

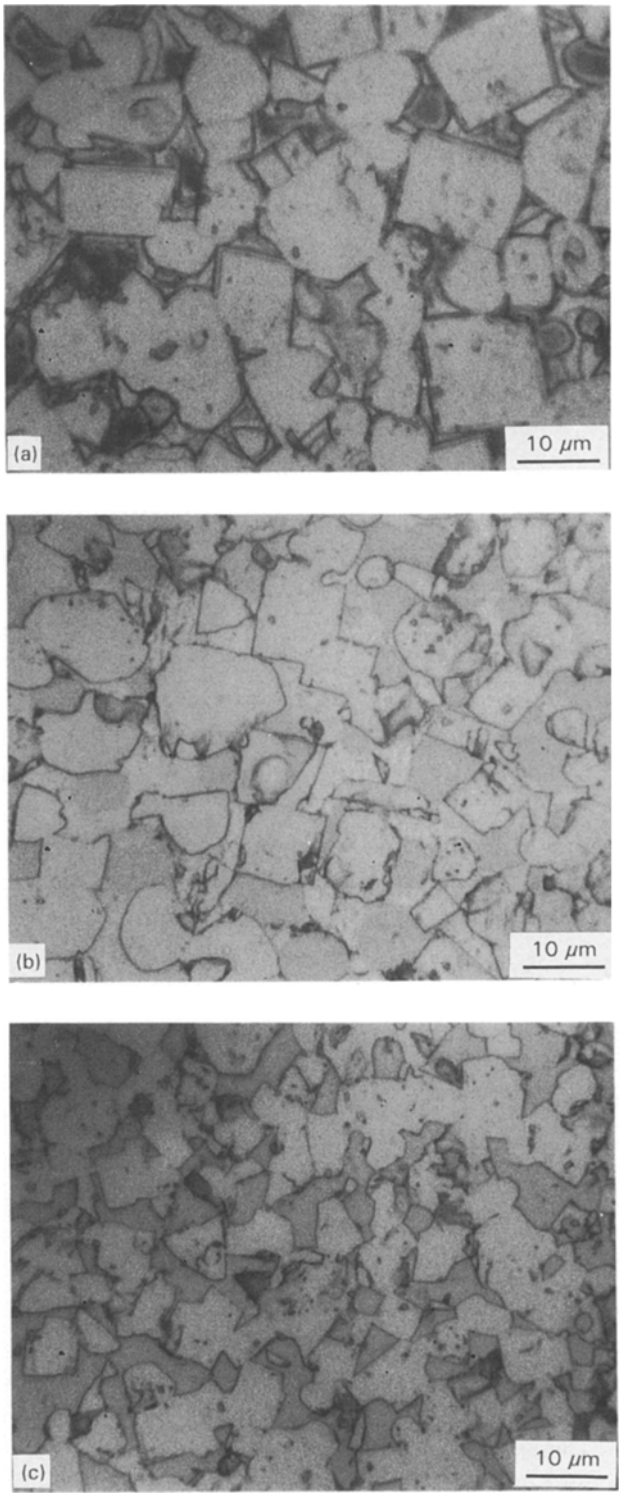

Figure 1 Optical micrographs of ZrB_2 composites fabricated by the reaction of ZrB_2 preform with the addition of (a) 10 vol % B_4C, (b) 20 vol % B_4C, (c) 30 vol % B_4C, for 10 min at 1900 °C.

Although platelet ZrB_2 was sometimes found in the large gap between the grains, most of the ZrB_2 and ZrC grains exhibited equi-shapes. These final phases are similar to the result observed in the direct reaction of molten zirconium with boron carbide. However, the shapes of the ZrB_2 grains in this study were different from those of the ZrB_2 grains in the specimens obtained by the direct reaction [9, 10]. Most of ZrB_2 grains in this study exhibited rectangular shapes, while they revealed platelet shapes in the direct reaction.

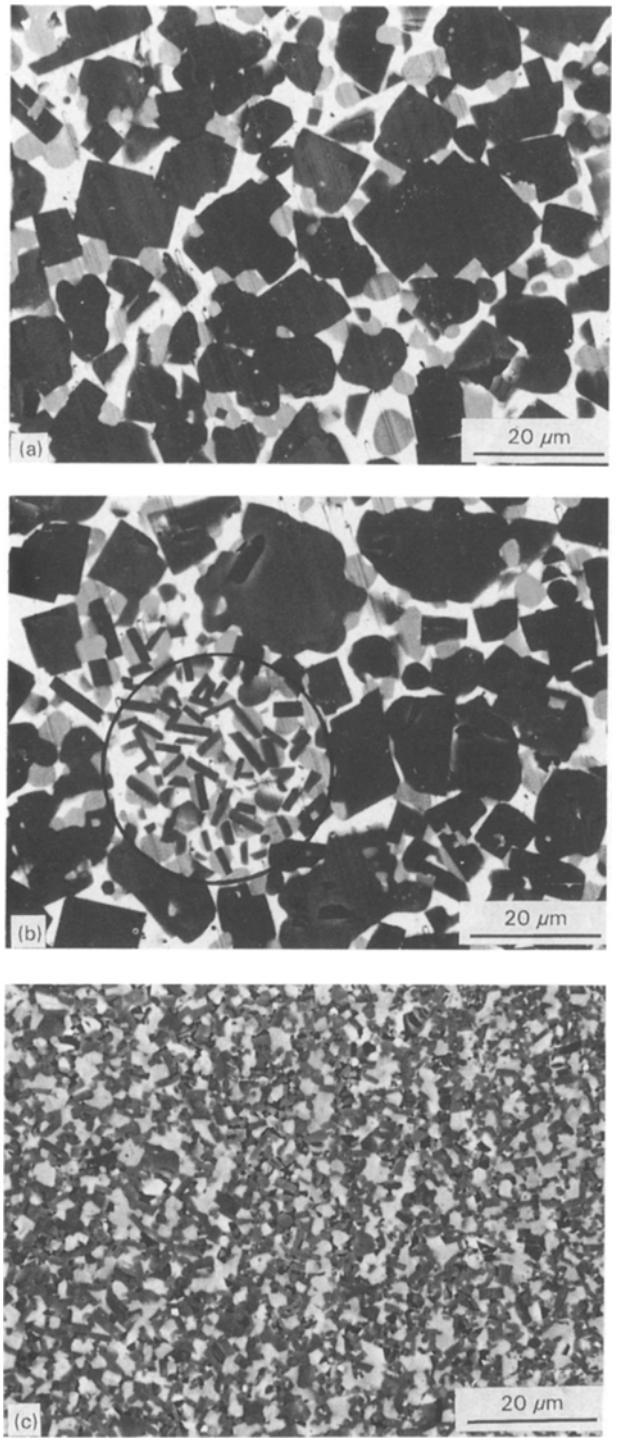

Figure 2 BEIs of the composite specimen made with ZrB_2–15 vol % B_4C preform infiltrated by zirconium for 10 min at 1900 °C. The darkest phase is ZrB_2, the grey phase is ZrC, and the white phase is zirconium metal.

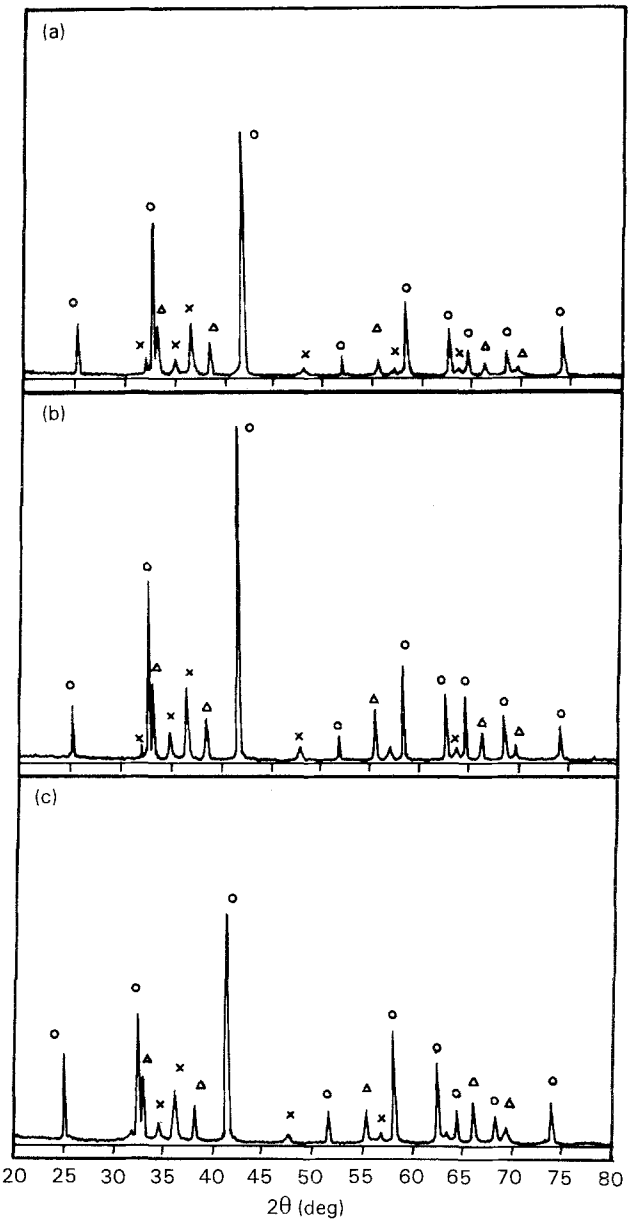

Figure 3 XRD patterns of composite specimens fabricated by the reaction of ZrB_2 preform with the addition of (a) 10 vol % B_4C, (b) 20 vol % B_4C, (c) 30 vol % B_4C, for 10 min at 1900 °C. (○) ZrB_2, (△) ZrC, (×) Zr.

X-ray diffractometry studies were conducted on flat, polished sections, and the patterns are shown in Fig. 3. The X-ray analysis showed the presence of three phases, such as ZrB_2, ZrC, and zirconium phase, in all the specimens investigated. No significant line broadening was observed in any of the X-ray diffraction peaks. This agrees well with the results of the BEIs of the ZrB_2–15 vol % B_4C preform infiltrated by zirconium as shown in Fig. 2. Also, it could be observed that the main intensity peak of ZrC was in the range $33° < 2\theta < 34°$. These suggested that zirconium carbide might be a stoichiometric compound (ZrC), while it was $ZrC_{0.6}$ in the directed reaction [9, 10].

It could be thought that the shape and phase differences came from different reaction mechanisms. That is, the reaction mechanism of this system seemed to be different from that of the direct reaction of molten zirconium with boron carbide, but seemed to be the same as that of the reaction-bonded silicon carbide [7, 8]. Therefore, the reaction mechanism was deduced to be the precipitation of β-SiC from a solution of graphite in molten silicon. The reaction begins as soon as the molten zirconium is sufficiently fluid to allow it to rise through the compact, its viscosity being initially quite high, but falling with increasing temperature. There is an exothermic reaction of molten zirconium with B_4C to form both ZrB_2 and ZrC, as previously reported [9, 10]. This exothermic reaction causes a local temperature rise at the dissolution sites and induces the activity gradient between boron, car-

bon and zirconium. The boron and carbon diffuse to locally cooler sites (original ZrB_2) where they become supersaturated in the zirconium. ZrB_2 and ZrC precipitate out to form the products, and these grains grow and deposit epitaxially on the original ZrB_2 by Ostwald ripening during processing [11].

The BEI micrographs have shown that ZrB_2 is present as rectangles of 10–20 μm width (Fig. 2a, b). These rectangular shapes were different from the platelet shape reported by Johnson *et al.* [9, 10]. Initially, ZrB_2 was platelet shaped, 2–3 μm diameter, as shown in Fig. 2c. Although platelet ZrB_2 was formed for the reaction between zirconium and boron carbide during the beginning of the reaction process, at the end of the reaction, the shape of ZrB_2 was changed to rectangular because newly formed ZrB_2 was epitaxially bonded to the original ZrB_2. After most of the new zirconium boride and zirconium carbide had formed, the exothermic reaction would begin to decay quite rapidly. Thus any remaining boron or carbon in solution would be precipitated out, as noted in the marked region of Fig. 2b. Thus, it could be concluded that the reaction mechanism in this system was an infiltration reaction similar to RBSC.

In order to evaluate the effect of B_4C content in the preform on the final microstructure of $ZrB_2/ZrC/Zr$ composites, the composites were made by infiltration of molten zirconium into ZrB_2 preform which contained 0–40 vol % B_4C at 1900 °C for 10 min.

Fig. 4 shows the BEIs of polished uncoated samples of $ZrB_2/ZrC/Zr$ composites. Capillary infiltration of the melt along the preform could be directly observed and took place in a matter of seconds. It revealed a dense microstructure of the composites, in which the zirconium almost filled up the pores. All of the specimens appeared approximately uniform and homogeneous. Furthermore, there was no freeze choking, but complete infiltration in all the specimens. Therefore, it could be concluded that the reaction rate was slower than the infiltration rate as reported earlier [9, 10].

Fig. 5 shows the bulk densities and the porosities of $ZrB_2/ZrC/Zr$ composites as a function of ZrC contents in the preform. The bulk densities of specimens was 6.18–6.20 g cm^{-3}, giving a calculated porosity ratio of 0.5%–0.25%. This density variation was associated with a variation in composition of 58 vol % ZrB_2, 42 vol % Zr to 60 vol % ZrB_2, 28 vol % ZrC, 12 vol % Zr in the composite specimens [8]. This porosity has also been confirmed by the method of point counting. It suggested that there were almost no pores in the specimens without pure ZrB_2. In the specimen without B_4C, infiltration behaviour was somewhat limited because zirconium had poor wettability for ZrB_2. However, the specimens with B_4C, had been fully densified, because chemical reactions between B_4C and zirconium could result in good wetting and enhance the infiltration [12].

The volume fractions of solid and liquid phases in the composites are shown in Fig. 6. The increase of

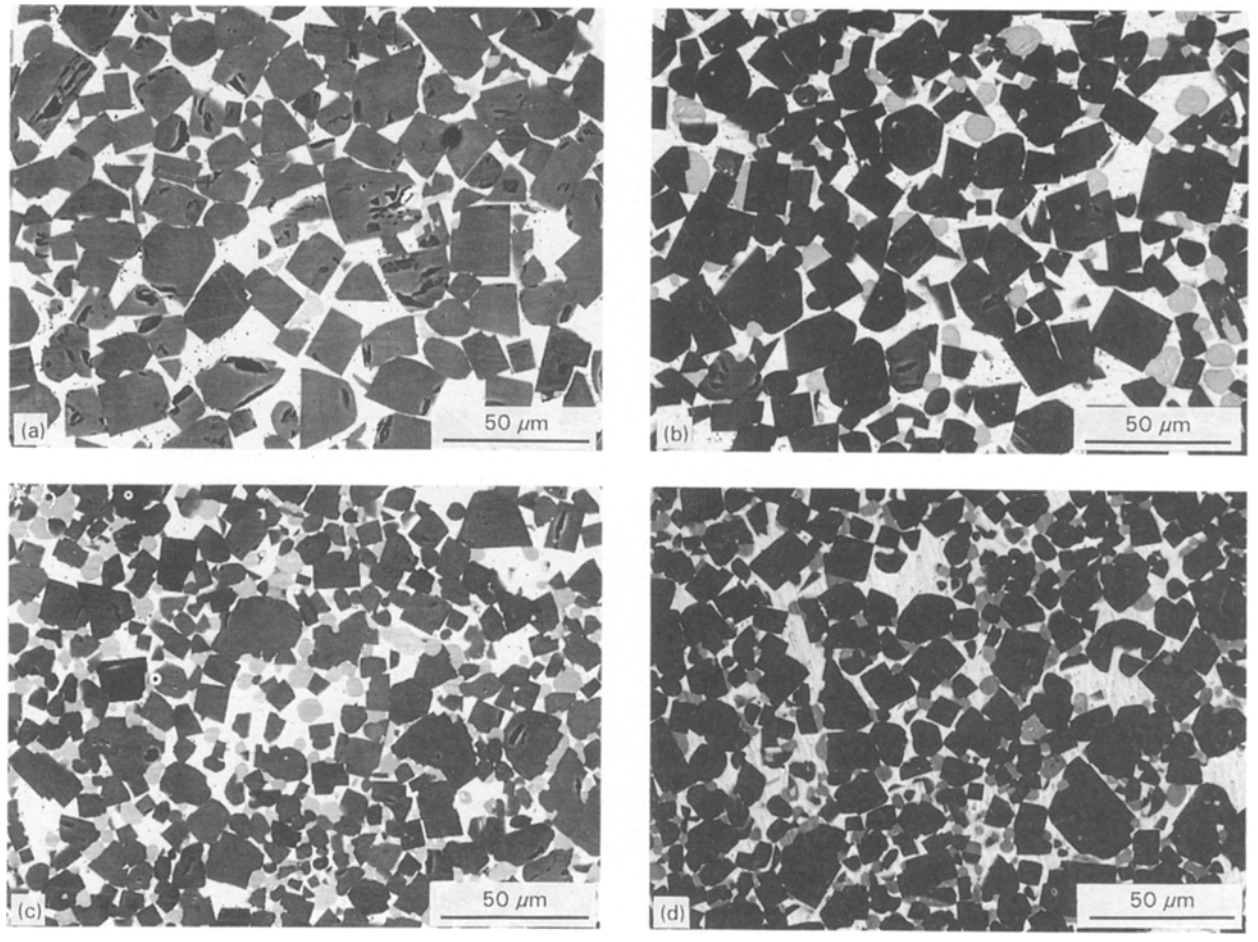

Figure 4 BEIs of ZrB_2 composites fabricated by the reaction of ZrB_2 preform with the addition of B_4C: (a) 0 vol %, (b) 5 vol %, (c) 10 vol %, (d) 15 vol %, (e) 20 vol %, (f) 30 vol %, (g) 40 vol %, with zirconium for 10 min at 1900 °C.

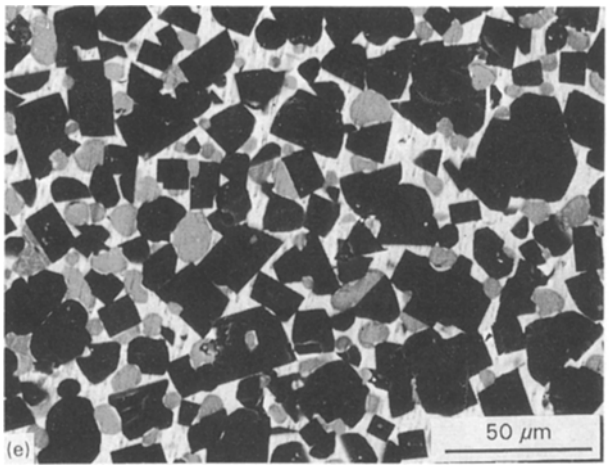

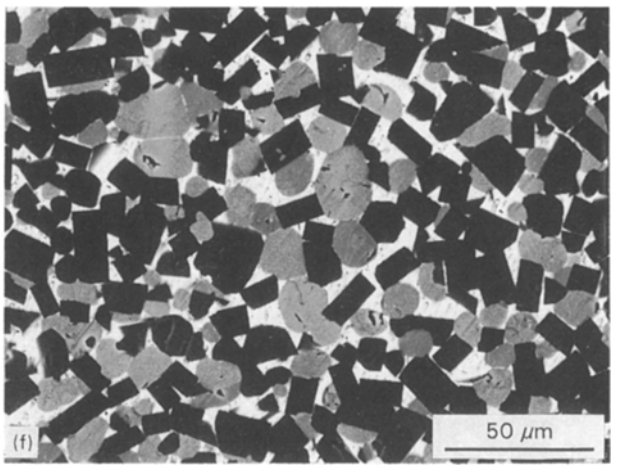

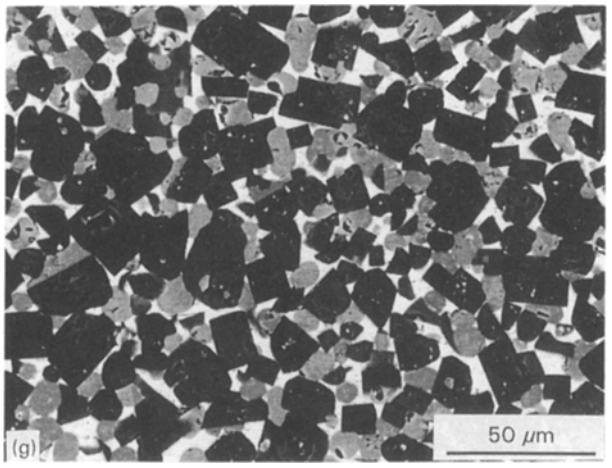

Figure 4 (continued).

B_4C content increased the solid (ZrB_2 and ZrC) contents. On the other hand, the zirconium content decreased as the B_4C content increased. As previously reported [9, 10], the predicted zirconium, ZrB_2, and ZrC contents are 2.6, 62.9, 34.5 vol % in the direct reaction of pure B_4C with zirconium. According to this result, it could be thought that the volume fraction of solid increased significantly with increase of the B_4C content. The increase of B_4C content in the preform increased the ZrC content in the composite monotonically. But the ZrB_2 content showed maximum value when the preform contained 15 vol % B_4C, and decreased with further increase of B_4C in the preform (Fig. 7).

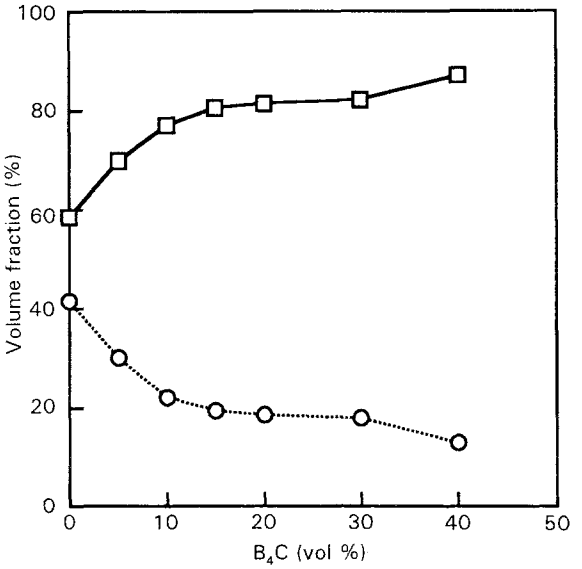

Figure 6 Volume fraction of (□) solid and (○) liquid versus B_4C content of ZrB_2 composites fabricated by the reaction of ZrB_2 preform with added B_4C and zirconium for 10 min at 1900 °C.

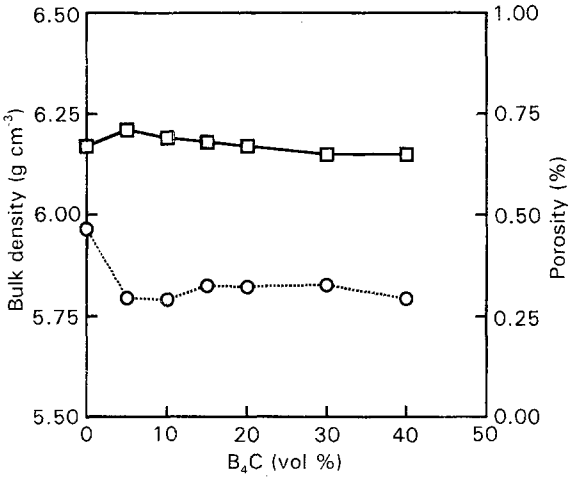

Figure 5 (□) Bulk density and (○) porosity ratio versus B_4C content of ZrB_2 composites fabricated by the reaction of ZrB_2 preform with added B_4C and zirconium for 10 min at 1900 °C.

The average grain sizes of ZrB_2 and ZrC obtained by reaction sintering for 10 min with various contents of B_4C are shown in Fig. 8. The microstructures shown in Fig. 4 suggested that the grain growth occurred so rapidly that ZrB_2 and ZrC grains became large grains in the relatively short reaction time. Such rapid grain growth could be caused by the presence of a liquid phase. The average grain size of original ZrB_2 was 2–3 μm (Fig. 2c) But, as the reaction proceeds, the average grain sizes of ZrB_2 and ZrC were 8–10 μm and 2–7 μm, respectively. As shown in Fig. 8, the average grain size of ZrB_2 slightly decreased with

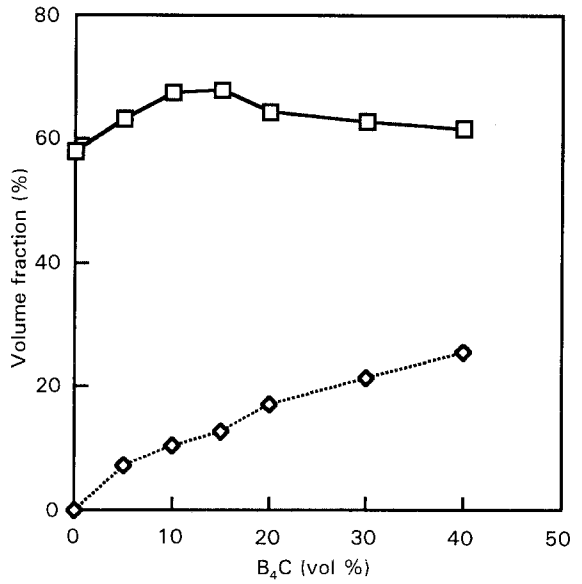

Figure 7 Volume fraction of (□) ZrB_2 and (◇) ZrC versus B_4C content of ZrB_2 composites fabricated by the reaction of ZrB_2 preform with added B_4C and zirconium for 10 min at 1900 °C.

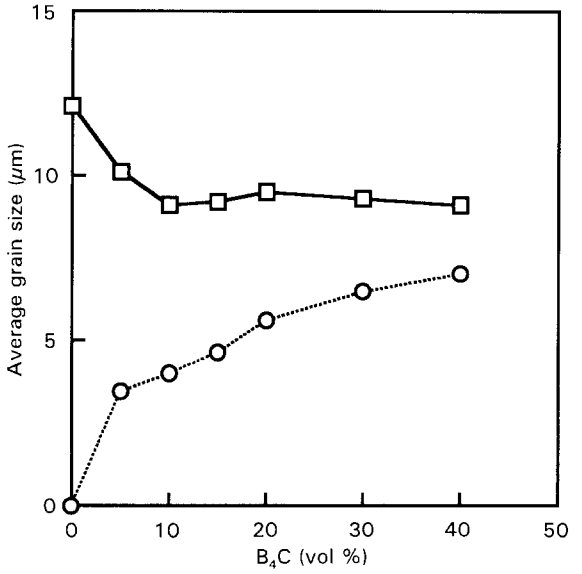

Figure 8 Average grain size of (□) ZrB_2 and (○) ZrC versus B_4C content of ZrB_2 composites fabricated by the reaction of ZrB_2 preform with added B_4C and zirconium for 10 min at 1900 °C.

further increase of B_4C content. It was thought that newly formed ZrC inhibited grain growth of ZrB_2 after all. On the other hand, in the case of ZrC, the average grain size increased with further increase of B_4C content. As the B_4C content increased, the ZrC content increased and the diffusion distance through the liquid became shorter. Therefore, the average grain size of ZrC increased with further increase of B_4C content.

The flexural strength and fracture toughness of the composites are summarized in Table I. The strength increased slightly in the ZrB_2–15 vol % B_4C specimen and then dropped gradually. It was thought that the increase of ZrB_2 content, as shown in Fig. 7, increases the fracture strength, and that the fracture strength of

TABLE I Flexural strength and fracture toughness of ZrB_2/ZrC/Zr composite as a function of B_4C content in the preform

B_4C content (vol %)	Flexural strength (MPa)	Fracture toughness ($MPa\,m^{1/2}$)
0	436	11.50
5	516	10.00
10	561	9.87
15	573	8.70
20	488	8.64
30	437	9.48
40	372	8.94

the specimen fell gradually because the volume fraction of ZrC was increased with increasing B_4C content [13]. These values are similar to other commercially available ceramics, but relatively lower than that of the direct reaction. It may be due to the larger grain size. The fracture toughness was in the range 8.4–11.5 $MPa\,m^{1/2}$, which is similar to that of the direct reaction. We could easily fabricate the ZrB_2/ZrC/Zr composites, which had various ZrB_2, ZrC, and zirconium contents and showed fracture toughness values of up to 11.5 $MPa\,m^{1/2}$ and fracture strengths of up to 570 MPa.

4. Conclusion

Dense ZrB_2/ZrC composites could be fabricated by the reaction sintering of molten zirconium with ZrB_2–B_4C preform. Infiltration and the reaction are essentially completed in a few minutes. It was thought that the reaction mechanism was infiltration followed by chemical reaction. It was found that the ZrB_2 was present as rectangular shapes. The volume fraction of solid was observed to increase with further increase of B_4C content. The average grain size of ZrB_2 in the reaction-sintered composites decreased slightly with increasing volume fraction of B_4C, but in the case of ZrC, the average grain size of ZrC was the opposite to ZrB_2. The flexural strength and fracture toughness of the composites were up to 11.5 $MPa\,m^{1/2}$ and up to 570 MPa, respectively.

References

1. C. F. POWELL, in "High Temperature Materials and Technology", edited by I. E. Campbell and E. H. Shenwood (Wiley, New York, 1967) p. 349.
2. W. C. TRIPP, H. H. DAVIS, and H. C. GRAHAM, *Am. Ceram. Soc. Bull.* **52** (1973) 612.
3. B. CECH, P. OLIVERIUS and J. SEJBAL, *Powder Metall.* **8** (15) (1965) 142.
4. M. A. KUZENKOVA and P. S. KISLYI, *Sov. Powder Metall. Met. Ceram.* **6** (1965) 479.
5. J. S. HAGGERTY and Y.-M. CHIANG, *Ceram. Eng. Sci. Proc.* **11** (1990) 757.
6. M. E. WASHBURN and W. S. COBLENZ, *Am. Ceram. Soc. Bull.* **67** (1988) 356.
7. P. POPPER, "Special Ceramics" (Heywood, London, 1960) p. 209.
8. C. W. FORREST, P. KENNEDY and J. V. SHENNAU, "Special Ceramics 5" (British Ceramics Research Association, Stoke-on-Trent, UK, 1972) p. 99.

9. W. B. JOHNSON, A. S. NAGELBERG and E. BREVAL, *J. Am. Ceram. Soc.* **74** (1991) 2093.
10. E. BREVAL and W. B. JOHNSON, *ibid.* **75** (1992) 2139.
11. Y. MASUDA and R. WATANABE, in "Sintering Processes", edited by Kuczynski (Plenum Press, New York, 1980) p. 3.
12. F. DELANNAY, L. FROYEM and A. DERUY TTERE, *J. Mater. Sci.* **22** (1987) 1.
13. T. D. CLAAR, W. B. JOHNSON, C. A. ANDERSSON and G. H. SCHIROKY, *Ceram. Eng. Sci. Proc.* **10** (1989) 599.

Received 23 February
and accepted 20 April 1994